Howard Hughes Medical Institute

Published as: *Environ Microbiol*. 2014 February ; 16(2): 417–429.

Architecture and host interface of environmental chlamydiae revealed by electron cryotomography

Martin Pilhofer[1,2,†], **Karin Aistleitner**[3,†], **Mark S. Ladinsky**[1], **Lena König**[3], **Matthias Horn**[3,*], and **Grant J. Jensen**[1,2,**]

[1]Division of Biology, California Institute of Technology, Pasadena, CA 91125, USA

[2]Howard Hughes Medical Institute, Pasadena, CA 91125, USA

[3]Division of Microbial Ecology, University of Vienna, Vienna, A-1090 Austria

Summary

Chlamydiae comprise important pathogenic and symbiotic bacteria that alternate between morphologically and physiologically different life stages during their developmental cycle. Using electron cryotomography, we characterize the ultrastructure of the developmental stages of three environmental chlamydiae: *Parachlamydia acanthamoebae*, *Protochlamydia amoebophila* and *Simkania negevensis*. We show that chemical fixation and dehydration alter the cell shape of *Parachlamydia* and that the crescent body is not a developmental stage, but an artefact of conventional electron microscopy. We further reveal type III secretion systems of environmental chlamydiae at macromolecular resolution and find support for a chlamydial needle-tip protein. Imaging bacteria inside their host cells by cryotomography for the first time, we observe marked differences in inclusion morphology and development as well as host organelle recruitment between the three chlamydial organisms, with *Simkania* inclusions being tightly enveloped by the host endoplasmic reticulum. The study demonstrates the power of electron cryotomography to reveal structural details of bacteria–host interactions that are not accessible using traditional methods.

Introduction

All chlamydiae share an obligate intracellular life style and depend on a eukaryotic host for replication (Horn, 2008). Chlamydial ancestors adapted to this life inside a host more than 700 million years ago probably thriving in ancient protists (Horn and Wagner, 2004; Horn *et al.*, 2004; Kamneva *et al.*, 2012; Subtil *et al.*, 2013). For a long time *Chlamydiae* were thought to consist of only human and certain animal pathogens (the *Chlamydiaceae*). In the past two decades, a novel class of ‘environmental’ chlamydiae have been identified in contaminated cell cultures, in an aborted bovine fetus, in fish gills, and as symbionts of arthropods and amoebae (Rourke *et al.*, 1984; Michel *et al.*, 1994; Kahane and Friedman,

[*]For correspondence. horn@microbial-ecology.net; Tel. (+43) 1 4277 76608; Fax (+43) 1 4277 876601. [**] jensen@caltech.edu; Tel. (+1) 626 395 8827; Fax (+1) 395 5730.
[†]Contributed equally.

Supporting information
Additional Supporting Information may be found in the online version of this article at the publisher’s web-site.

1995; Amann *et al.*, 1997; Rurangirwa *et al.*, 1999; Fritsche *et al.*, 2000; Horn *et al.*, 2000; Draghi *et al.*, 2004; Kostanjsek *et al.*, 2004; Thomas *et al.*, 2006; Karlsen *et al.*, 2008). While pathogenic chlamydiae are a homogeneous phylogenetic group, the genomes of environmental chlamydiae are more diverse (Bertelli *et al.*, 2010; Collingro *et al.*, 2011). It is still unclear to what extent this genomic variation manifests as variations in cell structure.

The biphasic chlamydial life cycle starts with the infection of a host cell by the elementary body (EB) (Horn, 2008). After uptake by the host, the EB resides inside a host-derived vacuole (termed 'inclusion') (Hackstadt *et al.*, 1997) and differentiates into a reticulate body (RB), the replicative developmental stage. The RB then divides several times by binary fission before redifferentiating into EBs, which leave the host cell by lysis or exocytosis to start a new round of infection (Abdelrahman and Belland, 2005; Hybiske and Stephens, 2007; Horn, 2008). An additional infectious developmental stage, the sickle-shaped crescent body, was reported for a number of environmental chlamydiae (Greub and Raoult, 2002; Lamoth and Greub, 2010; Nakamura *et al.*, 2010).

Once inside their host, chlamydiae perturb the organelle organization of the host cell in various ways. *Chlamydia trachomatis* inclusions, for instance, cause fragmentation of the Golgi (Heuer *et al.*, 2009), which facilitates the acquisition of cholesterol and sphingomyelin (Hackstadt *et al.*, 1995; Carabeo *et al.*, 2003). They also recruit the host's rough endoplasmic reticulum (rER), eventually resulting in a translocation of rER proteins into the inclusion (Dumoux *et al.*, 2012). Mitochondria are recruited to the inclusions of *C. psittaci* and *Waddlia chondrophila* (Friis, 1972; Peterson and de la Maza, 1988; Matsumoto *et al.*, 1991; Croxatto and Greub, 2010).

Internalization, inclusion development and host-organelle recruitment are all mediated by the secretion of effector proteins into the inclusion membrane and/or host cytoplasm by the type III secretion (T3S) system (Peters *et al.*, 2007). While the genes that encode this needle-like secretion system are present in all chlamydial genomes (Collingro *et al.*, 2011), T3S structures have not been seen in environmental chlamydiae, and few structural details are known about the T3S systems of pathogenic chlamydiae (Matsumoto, 1979; Nichols *et al.*, 1985; Dumoux *et al.*, 2012).

Studying chlamydial cell biology is challenging because of their obligate intracellular lifestyle and the lack of routine genetic tools (Binet and Maurelli, 2009; Kari *et al.*, 2011; Wang *et al.*, 2011; Nguyen and Valdivia, 2012). While many insights have come from conventional electron microscopy (EM) studies, the chemical fixation, dehydration, plastic embedding, thin sectioning and heavy-metal staining involved can lead to membrane artefacts, misleading representations of the nucleoid structure or loss of entire cellular components (Pilhofer *et al.*, 2010). Here, we investigated three environmental chlamydiae, *Protochlamydia amoebophila*, *Parachlamydia acanthamoebae* and *Simkania negevensis*, by electron cryotomography (ECT), which allows cells to be imaged in a near-native, 'frozen-hydrated' state. This approach revealed not only new structural details of these obligate intracellular bacteria at macromolecular resolution and in three dimensions but also provided new perspectives on the bacteria-host interface.

Results

Developmental stages of environmental chlamydiae

To investigate the ultrastructure of isolated cells, chlamydiae were purified from amoeba cultures, plunge-frozen on EM grids and imaged intact. Twenty-five, twenty and twenty tomograms were collected on purified *Simkania*, *Parachlamydia* and *Protochlamydia* cells respectively. EBs and RBs could be distinguished by their size, morphology and the granularity of their cytoplasm. EBs were coccoid and had diameters of 450 nm (*Simkania*, ±22, $n = 9$), 678 nm (*Parachlamydia*, ±32, $n = 5$) and 625 nm (*Protochlamydia*, ±170, $n = 5$) (Fig. 1A, D and G). RBs were more pleomorphic and larger (667 nm, *Simkania*, ±46, $n = 5$; 838 nm, *Parachlamydia*, ±135, $n = 4$; 884 nm, *Protochlamydia*, ±88, $n = 6$) (Fig. 1C, F and I). EBs exhibited regions of concentrated filamentous material (presumably condensed DNA), with different texture from the rest of the EB cytoplasm. Smaller but otherwise similar regions were also occasionally seen in RBs. Because of an irregularly shaped outer membrane, the thickness of the RB periplasm was more variable than that seen in EBs. Large numbers of ribosomes were found throughout the cytoplasm of both EBs and RBs except in the region of the putatively condensed DNA within EBs. We also observed cells with features characteristic of both developmental stages (Fig. 1B, E and H), including multiple small patches of condensed DNA, probably representing intermediate stages in the process of differentiation or redifferentiation.

Previous studies using conventional EM have reported that some chlamydiae exhibit crescent shapes, and these ‘crescent bodies’ were suggested to represent an infectious life stage of *Simkania*, *Parachlamydia* and *Protochlamydia* (Greub and Raoult, 2002; Lamoth and Greub, 2010; Nakamura *et al.*, 2010). Surprisingly, while our tomograms of intact as well as cryosectioned cells (see later) allowed for the identification of EBs, RBs and intermediate stages (Fig. 1), we never saw any crescent bodies (Fig. 1, Fig. 2A and B, Figs 3–5). We therefore explored if crescent bodies could be an artefact of chemical fixation and dehydration/embedding.

Parachlamydia cells were purified from asynchronous amoeba cultures and split into two aliquots. One sample was processed with procedures similar to the original study describing crescent bodies (Greub and Raoult, 2002): cells were fixed with glutaraldehyde and osmium tetroxide, dehydrated, plastic-embedded, thin-sectioned, stained and imaged at room temperature. Crescent bodies made up 47 ± 10% of all putative chlamydial cells ($n = 813$) and had the typical shape and dimensions reported previously (Greub and Raoult, 2002) (arrows in Fig. 2C and D). The second sample was treated in the same way, except that the osmolarity and fixative concentration in the fixation buffer was reduced. Crescent bodies were still present but only at a frequency of 2 ± 2% ($n = 1355$) (Fig. 2E). Osmolarity and fixative concentration therefore influence the abundance of crescent bodies. This was further supported by scanning EM (SEM) of purified chlamydial cells, where buffers with higher osmolarity and higher fixative concentration also resulted in an increased percentage of crescent bodies (Fig. 2F).

To distinguish between the effects of fixation and dehydration/plastic embedding, two further aliquots of purified cells were cryopreserved (i.e. plunge-frozen) and imaged in a

frozen-hydrated state in an electron cryomicroscope. No crescent bodies were found in projection images of 584 cells, which were directly plunge-frozen after purification (Movie S1). When cells were fixed with glutaraldehyde and osmium tetroxide before plunge-freezing, crescent bodies were still absent (data not shown). Lysed cells were observed in some cases, but none of those had a typical crescent shape or continuous intact membranes, which are characteristic for crescent bodies. We conclude that crescent bodies are an artefact of the combined effect of chemical fixation and dehydration/embedding.

Architecture of inclusions

Next chlamydiae were imaged inside their host. Because ECT is limited to thin (less than ~500 nm) samples, asynchronously infected amoeba cultures were pelleted, mixed with cryoprotectant, high-pressure frozen, sectioned at cryotemperatures (150 nm section thickness) and then imaged. Twenty-one, four and twenty-seven tomograms were collected of vitreous cryosections of *Simkania*-, *Parachlamydia*- and *Protochlamydia*-infected amoebae respectively. For comparison, we also collected tomograms of parallel samples prepared by high-pressure freezing, freeze-substitution, plastic-embedding, thin-sectioning and staining.

First, the localization of chlamydiae inside their host was investigated. Intracellular bacterial cells were always seen surrounded by an inclusion membrane and never directly in the cytoplasm (Figs 3 and 4, and Movies S2, S3 and S4). Single-celled inclusions and inclusions packed with up to 17 chlamydial cells were observed in amoebae infected with *Simkania* (Fig. 3A–F) or *Parachlamydia* (Fig. 3G–L). RBs were the predominant stage within the inclusions, some of them dividing by binary fission. In contrast, 92% ($n = 52$) of the inclusions in amoebae infected with *Protochlamydia* contained a single bacterial cell (Fig. 4A, D and E). The 8% of inclusions harbouring more than one bacterium were not roundish and tightly packed with bacteria, as seen for *Parachlamydia* and *Simkania* (Fig. 3); they rather appeared like inclusions in the process of starting separation, with membranes contracting in between the bacteria (Fig. 4B and C), or in a stage where two single-cell inclusions were connected by a narrow membrane tube (the percentage of single-cell inclusions in all cases might actually be slightly lower than noted, as extensions of the inclusions above and below the section cannot be visualized).

Interestingly, we observed a difference in cell shape between *Simkania* EBs imaged inside densely packed inclusions within their host versus after purification. While EBs imaged inside these inclusions were frequently rod-shaped or elongated (cells labelled ‘EB’ in Figs 3F and 5A), purified EBs were always spherical (Fig. 1A). *Parachlamydia* and *Protochlamydia* EBs, in contrast, were always coccoid (Fig. 1D and G, and cells labelled ‘EB’ in Fig. 5B and C). RBs of all species had a somewhat polymorphic, spherical shape inside the host cell.

Recruitment of ER by Simkania

Chlamydiae associate not only with the inclusion membrane, but some also recruit and reshape entire host organelles. We found that inclusions of *Simkania* were always enveloped by an additional membranous structure (Fig. 3A–F). The granularity inside the cisternae-like

membrane sacs was different from the rest of the eukaryotic cytoplasm, suggesting that they were part of a separate compartment. The endoplasmic reticulum (ER)-like membrane architecture and the presence of many ribosomes on the cytoplasmic side of the distal membrane identified the compartment as rER. Segmentations showed that the inclusions were not entirely surrounded by the rER, however, leaving small patches of direct connections between inclusion and amoeba cytoplasm (Fig. 3D). rER was found associated with single-cellular (Fig. 3A, B and E) and multicellular inclusions filled with EBs and RBs (Fig. 3C and F), indicating that ER recruitment occurs early after internalization and remains throughout the intracellular stage.

In contrast with *Simkania*, no direct association of *Parachlamydia* or *Protochlamydia* inclusions and any host organelle was detected. Mitochondria were occasionally observed in their vicinity (Figs 3G–L and 4A–E), but a specific co-localization was not suggested by fluorescent labelling of mitochondria (Fig. S1).

Secretion systems

Translocation of chlamydial effector proteins into the inclusion membrane and into the host cytoplasm is crucial for chlamydiae to shape their intracellular environment. In a cryotomogram of a *Simkania* EB, we observed a structure with characteristics typical of a T3S apparatus (Fig. 6A and B) (Marlovits *et al.*, 2004). A density in the periplasm was found to be similar to T3S basal bodies and connected to an extracellular needle-like structure. The needle (length 63 nm, diameter 9 nm) seemed to be engaged with a membranous structure, possibly a remnant of the host cell. The dimensions of the apparatus were similar to projections seen on the surface of infectious *C. psittaci* cells (Matsumoto, 1979). Interestingly, the otherwise relatively narrow distance between the inner and outer membrane (13 nm) in *Simkania* EBs required a bulging (41 nm) of the cytoplasmic membrane to accommodate the basal body. Such widening of the periplasm was observed frequently in the same and other EBs (Figs 6A and S2). Basal body-like densities inside these bulges indicate that they likely represented T3S structures as well, but the corresponding needles were probably sheared off during purification. A pronounced widening of the periplasmic space was also reported for T3S structures of *C. trachomatis* (Dumoux *et al.*, 2012).

Putative T3S systems in *Parachlamydia* showed a similar bulging of the periplasm in the region of the basal body (36–44 nm rather than 17 nm) (Fig. 6C–F). The needle structure was substantially different compared with *Simkania*, with a length of 38–42 nm, a diameter of 6–7 nm and a widening (12 nm) of the needle 7 nm from its tip (Fig. 6D and F). A T3S-like structure found on a *Protochlamydia* EB comprised a 52-nm-long, 7-nm-diameter needle, and may have also had a widening close to the needle tip (Fig. 6G and H). Periplasmic bulging was not observed, however, as the width of the periplasm in *Protochlamydia* was already ~40 nm.

Discussion

EBs and RBs in a life-like state

Early conventional EM studies suggested that the DNA in EBs is condensed (Moulder, 1966), which was later found to be mediated by histone-like proteins (Barry *et al.*, 1992). However, nucleoid structure in particular is prone to artefacts introduced by fixation, dehydration and staining in conventional EM (Pilhofer *et al.*, 2010). While a more recent ECT study imaged *C. trachomatis* cells preserved in a near-native, frozen-hydrated state, such ultrastructural details were unfortunately not resolved probably due to instrumental limitations (Huang *et al.*, 2010). Again plunge-freezing cells, but using higher electron energies and energy filtration, here we have confirmed that EB genomes are indeed densely packed. Our finding of ribosomes in EBs is consistent with the notion that they are metabolically active to some degree (Haider *et al.*, 2010; Sixt *et al.*, 2013) rather than completely dormant (Hatch *et al.*, 1985). Besides size differences of EBs and RBs not observed before for environmental chlamydiae, another distinguishing feature between the developmental stages we noted was the variable periplasmic width in RBs. This is consistent with the notion that lower abundances of stabilizing cysteine-rich proteins in RBs result in more flexible outer membranes (Hatch *et al.*, 1986). Similarly, the more flexible shape and deformation of *Simkania* EBs inside host cells compared with *Protochlamydia* and *Parachlamydia* might be a consequence of differences in cell envelope architecture, such as the absence of the cysteine-rich proteins that *Simkania* lacks in contrast with all other chlamydiae (Collingro *et al.*, 2011).

Crescent bodies are an artefact

While crescent-shaped cells had been seen previously and thought to represent a distinct developmental stage (Greub and Raoult, 2002; Lamoth and Greub, 2010; Nakamura *et al.*, 2010), here we showed that they are artefacts of conventional EM methods. While no crescent bodies have been reported for the pathogenic *Chlamydiaceae*, EBs with peculiar stellate outlines were found occasionally. The previous hypothesis that this morphology could be attributed to EM preparation methods as well (Matsumoto, 1988) is supported by our results. The reason for crescent bodies not being observed in *Chlamydiaceae* could be differences in their outer membrane protein composition compared with environmental chlamydiae (Heinz *et al.*, 2009; Collingro *et al.*, 2011), leading to different effects during chemical fixation and dehydration/embedding.

Trapezoidal, dumbbell-shaped and elongated intracellular *Simkania* EBs have also been described in the past (Kahane *et al.*, 2001; Michel *et al.*, 2005; Henning *et al.*, 2007). While we found elongated morphologies especially in cells tightly packed in inclusions, trapezoidal and dumbbell-shaped forms were never seen, suggesting that those are also artefacts. Conventional EM studies of other environmental chlamydiae EBs have reported head-and-tail, star and rod shapes (Kostanjsek *et al.*, 2004; Karlsen *et al.*, 2008; Lienard *et al.*, 2011). It remains unclear whether these morphologies are natural.

Shapes of bacteria from other phyla have also been reported to be affected by chemical fixation and dehydration. For instance, crescent-shaped cells were observed for *Gemmata*

obscuriglobus (Lindsay *et al.*, 1995), a member of the chlamydial sister-phylum *Planctomycetes*, and the mollicute *Acholeplasma ladlawii* (Lemcke, 1972), showing that fixation conditions must be chosen carefully to preserve the cell shape and that the description of new shapes based on fixed cells should be handled with caution.

Diversity of the intracellular niche of environmental chlamydiae

Most chlamydiae are known to reside inside the host-derived membranous inclusion after host cell invasion (Hackstadt *et al.*, 1997), but *Parachlamydia* and *Simkania* have also been reported to be localized directly in the cytoplasm (Michel *et al.*, 1994; Greub and Raoult, 2002). Here, intracellular chlamydiae were always seen surrounded by an inclusion membrane, supporting the importance of this host-bacterium interface for intracellular survival and replication. Inclusions in *Protochlamydia* infections were exclusively unicellular, but *Simkania* and *Parachlamydia* cells were more commonly found in multicellular inclusions.

Some chlamydial species are known to recruit and reshape entire host organelles including mitochondria, Golgi stacks or the ER (Peterson and de la Maza, 1988; Matsumoto *et al.*, 1991; Heuer *et al.*, 2009; Croxatto and Greub, 2010; Dumoux *et al.*, 2012). We found that *Simkania* inclusions are almost entirely enveloped by the rER (Fig. 3), adding additional layers to the host-bacterial interface. In this way, *Simkania* might use a similar strategy as the facultative intracellular pathogens *Legionella pneumophila* and *Brucella abortus* (Swanson and Isberg, 1995; Abu Kwaik *et al.*, 1998; Roy, 2002). However, in contrast with *L. pneumophila* and *B. abortus* phagosomes, the *Simkania* inclusion does not fuse with ER-derived vesicles, and *Simkania* thus remains inside the inclusion. The tight association of the *Simkania* inclusion with the ER could nevertheless provide similar benefits such as prevention from fusing with lysosomes. Interestingly, the abilities to recruit ER and to replicate in human and insect cells coincide in *Simkania* (Kahane *et al.*, 2007; Sixt *et al.*, 2012) and members of the pathogenic chlamydiae (Dumoux *et al.*, 2012), but are absent in *Parachlamydia* and *Protochlamydia*.

Species-specific differences in inclusion morphology and recruitment of host organelles are likely due to the presence of different effector proteins in the inclusion membrane (Rockey *et al.*, 1997; Betts *et al.*, 2009; Heinz *et al.*, 2010). Adaptation to different hosts likely drove the diversification of environmental chlamydiae (Bertelli *et al.*, 2010; Collingro *et al.*, 2011).

T3S systems

Translocation of chlamydial effector proteins through the elaborate cell envelope and the inclusion membrane requires a secretion system and is thought to be accomplished by the T3S system. T3S systems are encoded in all known chlamydial genomes (Peters *et al.*, 2007; Collingro *et al.*, 2011), and T3S proteins were detected during all stages of infection in members of the pathogenic chlamydiae (Fields *et al.*, 2003). For the first time, we detected T3S-like structures in environmental chlamydiae, providing evidence for its conservation and crucial role in the infectious life cycle of modern and likely ancient chlamydiae. Fewer T3S-like structures were observed by ECT in environmental chlamydiae than by

conventional transmission electron microscopy in pathogenic chlamydiae (Matsumoto, 1982; Wilson *et al.*, 2006).

T3S needle tip proteins in other bacteria are known to be highly adapted to the host (Abby and Rocha, 2012). It has been unclear whether the chlamydial T3S needle harbours a tip protein at all. To date, only one candidate for a chlamydial needle tip protein has been identified, but it remains unclear whether it rather functions as an effector (Markham *et al.*, 2009; Stone *et al.*, 2012). The subterminal widening of the needle in *Parachlamydia* and *Protochlamydia* seen here indicates that the chlamydial T3S apparatus likely does include a needle tip protein. Interestingly, T3S structures were not seen on purified or cryosectioned RBs perhaps because the juxtaposition of the RB outer membrane and inclusion membrane effects the length of the needle.

Imaging bacteria–host interactions in a near-native state

Finally, this is the first study to image bacteria inside their host in a near-native, frozen-hydrated state. In addition to avoiding and uncovering artefacts, this approach provided novel insights into the nature of the host-bacterial interface. Because amoebae can also serve as hosts for important pathogens such as *Legionella pneumophila*, *Vibrio cholerae*, mycobacteria, *Francisella tularensis*, *Pseudomonas aeruginosa* and *Helicobacter pylori* as well as bacterial symbionts like *Amoebophilus asiaticus*, *Paracaedibacter symbiosus* or *Procabacter acanthamoebae* (Horn and Wagner, 2004; Schmitz-Esser *et al.*, 2008), our approach should prove helpful in the study of many other important bacteria–host interactions in the future.

Experimental procedures

Cultivation of organisms and staining of mitochondria

Acanthamoeba castellanii UWC1 infected with *Parachlamydia acanthamoebae* UV7 or *Simkania negevensis* and *A. castellanii* Neff infected with *Protochlamydia amoebophila* UWE25 were cultivated in TSY (trypticase soy broth with yeast extract) medium (30 g l^{-1} trypticase soy broth, 10 g l^{-1} yeast extract, pH 7.3) at 20°C. Amoebal growth was monitored by light microscopy and medium was exchanged every 3–6 days. The presence and identity of the chlamydial symbionts was checked regularly by fluorescence *in situ* hybridization (FISH) combined with 4′,6-diamidino-2-phenylindole staining of infected cultures using specific probes for the respective symbiont as described previously (Schmitz-Esser *et al.*, 2008). In addition, the identity of the symbionts was verified by isolation of DNA from cultures followed by amplification and sequencing of the 16S rRNA genes. For staining of mitochondria, *A. castellanii* infected with chlamydial symbionts were incubated with 2 μM MitoTracker Orange CMTMRos (Molecular Probes) in TSY for 45 min. Cells were fixed with 4% paraformaldehyde, followed by FISH with specific probes.

Purification of chlamydiae

Infected *A. castellanii* cultures were harvested by centrifugation (7197 × *g*, 10 min), washed in Page's amoebic saline (PAS) (Page, 1976), centrifuged and resuspended in PAS. Amoeba cells were ruptured by vortexing with an equal volume of glass beads for 3 min. Glass beads

and cell debris were removed by centrifugation (5 min, 300 × *g*). The supernatant was filtered through a 1.2 μm filter and centrifuged at maximum speed for 10 min. The obtained pellet was resuspended in PAS.

Conventional transmission EM

To analyse the impact of fixation and to compare the effect of different fixation buffers on the morphology of *Parachlamydia*, chlamydiae were purified from their amoeba hosts, and the sample was divided into three parts. One part was immediately plunge-frozen (see later). The second part was fixed in 4% glutaraldehyde in phosphate buffered saline (PBS, 130 mM NaCl, 10 mM Na_xPO_4; pH 7.2–7.4) for 1 h, washed in PBS and further fixed in 1% osmium tetroxide in PBS for 1 h followed by two washing steps. The third part was fixed in the same way as the second sample, except that 2% glutaraldehyde in phosphate buffer (10 mM Na_xPO_4; pH 7.2–7.4) was used as first fixative and that the 10 mM phosphate buffer replaced PBS in the following washing and fixation steps. Samples were dehydrated in ethanol and acetone through a graded series, embedded in Epon-Araldite (Electron Microscopy Sciences, Port Washington, PA), thin-sectioned with a UC6 ultramicrotome (Leica, Vienna, Austria), and stained with uranyl acetate and lead citrate. Two-dimensional images were recorded on a Tecnai T12 TEM (FEI, Eindhoven, the Netherlands).

For room temperature EM of high-pressure frozen/freeze substituted samples, infected amoeba cells were high-pressure frozen (see later). The frozen domes were transferred under liquid nitrogen to cryotubes containing 2% or 0.04% glutaraldehyde in acetone. The tubes were placed in a model AFS freeze-substitution machine (Leica) and freeze-substituted at −90°C for 60 h, then warmed to −20°C over 10 h. Cells were rinsed 3× with cold acetone, then post-fixed with 2.5% osmium tetroxide in acetone at −20°C for 24 h. The samples were then warmed to 4°C over 2 h, rinsed 3× with cold acetone, and embedded in Epon-Araldite resin (Electron Microscopy Sciences). Following polymerization, semi-thin (200 nm) sections were cut with a UC6 ultramicrotome (Leica) and placed on Formvar-coated, copper/rhodium 1 mm slot grids (Electron Microscopy Sciences). Sections were stained with uranyl acetate and lead citrate, and imaged in a Tecnai T12 TEM (FEI). Dual-axis tilt-series were acquired using SerialEM (Mastronarde, 2005), then subsequently calculated and analysed using IMOD (Kremer *et al.*, 1996) on an Apple MacPro computer.

Plunge-freezing

For plunge-freezing, copper/rhodium EM grids (R2/2 or R2/1, Quantifoil, Jena, Germany) were glow-discharged for 1 min. A 20×-concentrated bovine serum albumin-treated solution of 10 nm colloidal gold (Sigma, St Louis, MO) was added to purified chlamydiae (1:4 v/v) immediately before plunge freezing. A 4 μl droplet of the mixture was applied to the EM grid, then automatically blotted and plunge-frozen into a liquid ethane-propane mixture (Tivol *et al.*, 2008) using a Vitrobot (FEI) (Iancu *et al.*, 2006).

Cryosectioning

Acanthamoeba castellanii cells continuously infected with either *Simkania*, *Parachlamydia* or *Protochlamydia* were mixed with uninfected amoeba cells at a ratio of 1:1 and incubated for 24 h. For *Parachlamydia*, the ratio of infected to uninfected cells was 5:1. Amoebae were

harvested (7197 × *g*, 10 min), and the pellet was mixed with 40% dextran (w/v) in PAS. The samples were transferred to brass planchettes and rapidly frozen in a HPM010 high-pressure freezing machine (Bal-Tec, Leica). Cryosectioning of the vitrified samples was done as previously described (Ladinsky *et al.*, 2006; Ladinsky, 2010). Semi-thin (90–200 nm) cryosections were cut at −145°C or −160°C with a 25°Cryo diamond knife (Diatome, Biel, Switzerland), transferred to grids (continuous carbon-coated 200-mesh copper grids or 700-mesh uncoated copper grids) and stored in liquid nitrogen.

ECT

Images were collected using a Polara 300 kV FEG transmission electron microscope (FEI) equipped with an energy filter (slit width 20 eV; Gatan, Pleasanton, CA) on a lens-coupled 4 k × 4 k UltraCam charge-coupled device (CCD) (Gatan) or K2 Summit direct electron detector (Gatan). Pixels on the CCD represented 0.95 nm (22 500×) or 0.63 nm (34 000×) at the specimen level. Typically, tilt series were recorded from −60° to +60° with an increment of 1° at 10 μm under-focus. The cumulative dose of a tilt-series was 180–220 e−/Å2 (for whole cells) or 100–150 e−/Å2 (for cryosections). UCSFTOMO (Zheng *et al.*, 2007) was used for automatic acquisition of tilt-series and two-dimensional projection images. Three-dimensional reconstructions were calculated using the IMOD software package (Kremer *et al.*, 1996) or Raptor (Amat *et al.*, 2008). Tomograms of cryosections were reconstructed using IMOD's patch tracking to generate the aligned stack (Kremer *et al.*, 1996). Tomograms were visualized and segmented using 3dMOD (Kremer *et al.*, 1996).

SEM

Glass coverslips (12-mm diameter) were cleaned in acidic ethanol, dried for 1 h at 60°C and coated with 0.01% poly-L-Lysine solution for 10 min. Two hundred microlitres of purified *Parachlamydia* in the respective buffer were spotted onto the dry coverslip. After 10 min non-attached cells were removed, and remaining cells were fixed for 1 h at room temperature using the following fixatives: 2% glutaraldehyde in 10 mM phosphate buffer (pH 7.2), 2.5% glutaraldehyde in 3 mM cacodylate buffer (pH 7.2), 2% glutaraldehyde in DGM-21A-defined medium (Haider *et al.*, 2010), 4% glutaraldehyde in 10 mM phosphate buffer with 130 mM NaCl, and 4% glutaraldehyde in 10 mM phosphate buffer with 260 mM NaCl. After three washing steps (5 min each) in the respective buffer, cells were further fixed in 1% osmium tetroxide in the respective buffer for 1 h at room temperature and washed again three times. Samples were dehydrated in acetone and chemically dried in hexamethyldisilazane. Glass slides were gold coated for 160 s using default settings (Agar sputter coater B7340) and analysed using a Philips XL-30 ESEM. For analysis, 10 or more random SEM images with 36 or more individual putative bacterial cells in total were taken. Roundish or crescent-shaped objects with a diameter of 0.5–1 μm were counted as bacterial cells. Each cell was then classified into one out of four morphological types (crescent shape, large invaginations, small invaginations, coccoid), and the percentage of each type was determined. Osmolarity measurements of buffers and fixatives were performed using an Advanced Micro 3MO plus osmometer (Block Scientific, New York, NY). Samples and standards were measured three times each.

Supplementary Material

Refer to Web version on PubMed Central for supplementary material.

Acknowledgments

This work was funded by the Austrian Science Fund FWF (Y277-B03 to MH), the European Research Council (ERC StG 'EvoChlamy' to MH), the Caltech Center for Environmental Microbiology Interactions (to GJJ, MP), and a gift from the Gordon and Betty Moore Foundation to Caltech.

References

Abby SS, Rocha EPC. The non-flagellar type III secretion system evolved from the bacterial flagellum and diversified into host-cell adapted systems. PLoS Genet. 2012; 8:e1002983. [PubMed: 23028376]

Abdelrahman YM, Belland RJ. The chlamydial developmental cycle. FEMS Microbiol Rev. 2005; 29:949–959. [PubMed: 16043254]

Abu Kwaik Y, Gao LY, Stone BJ, Venkataraman C, Harb OS. Invasion of protozoa by *Legionella pneumophila* and its role in bacterial ecology and pathogenesis. Appl Environ Microbiol. 1998; 64:3127–3133. [PubMed: 9726849]

Amann R, Springer N, Schonhuber W, Ludwig W, Schmid EN, Muller KD, Michel R. Obligate intracellular bacterial parasites of acanthamoebae related to *Chlamydia* spp. Appl Environ Microbiol. 1997; 63:115–121. [PubMed: 8979345]

Amat F, Moussavi F, Comolli LR, Elidan G, Downing KH, Horowitz M. Markov random field based automatic image alignment for electron tomography. J Struct Biol. 2008; 161:260–275. [PubMed: 17855124]

Barry CE, Hayes SF, Hackstadt T. Nucleoid condensation in *Escherichia coli* that express a chlamydial histone homolog. Science. 1992; 256:377–379. [PubMed: 1566085]

Bertelli C, Collyn F, Croxatto A, Ruckert C, Polkinghorne A, Kebbi-Beghdadi C, et al. The Waddlia genome: a window into chlamydial biology. PLoS ONE. 2010; 5:e10890. [PubMed: 20531937]

Betts HJ, Wolf K, Fields KA. Effector protein modulation of host cells: examples in the *Chlamydia* spp. arsenal. Curr Opin Microbiol. 2009; 12:81–87. [PubMed: 19138553]

Binet R, Maurelli AT. Transformation and isolation of allelic exchange mutants of *Chlamydia psittaci* using recombinant DNA introduced by electroporation. Proc Natl Acad Sci USA. 2009; 106:292–297. [PubMed: 19104068]

Carabeo RA, Mead DJ, Hackstadt T. Golgi-dependent transport of cholesterol to the *Chlamydia trachomatis* inclusion. Proc Natl Acad Sci USA. 2003; 100:6771–6776. [PubMed: 12743366]

Collingro A, Tischler P, Weinmaier T, Penz T, Heinz E, Brunham RC, et al. Unity in variety – the pan-genome of the *Chlamydiae*. Mol Biol Evol. 2011; 28:3253–3270. [PubMed: 21690563]

Croxatto A, Greub G. Early intracellular trafficking of *Waddlia chondrophila* in human macrophages. Microbiology. 2010; 156:340–355. [PubMed: 19926655]

Draghi A 2nd, Popov VL, Kahl MM, Stanton JB, Brown CC, Tsongalis GJ, et al. Characterization of '*Candidatus Piscichlamydia salmonis*' (order *Chlamydiales*), a chlamydia-like bacterium associated with epitheliocystis in farmed Atlantic salmon (*Salmo salar*). J Clin Microbiol. 2004; 42:5286–5297. [PubMed: 15528727]

Dumoux M, Clare DK, Saibil HR, Hayward RD. Chlamydiae assemble a pathogen synapse to hijack the host endoplasmic reticulum. Traffic. 2012; 13:1612–1627. [PubMed: 22901061]

Fields KA, Mead DJ, Dooley CA, Hackstadt T. Chlamydia trachomatis type III secretion: evidence for a functional apparatus during early-cycle development. Mol Microbiol. 2003; 48:671–683. [PubMed: 12694613]

Friis RR. Interaction of L cells and *Chlamydia psittaci*: entry of the parasite and host responses to its development. J Bacteriol. 1972; 110:706–721. [PubMed: 4336694]

Fritsche TR, Horn M, Wagner M, Herwig RP, Schleifer KH, Gautom RK. Phylogenetic diversity among geographically dispersed *Chlamydiales* endosymbionts recovered from clinical and

environmental isolates of *Acanthamoeba* spp. Appl Environ Microbiol. 2000; 66:2613–2619. [PubMed: 10831445]

Greub G, Raoult D. Crescent bodies of *Parachlamydia acanthamoebae* and its life cycle within *Acanthamoeba polyphaga*: an electron micrograph study. Appl Environ Microbiol. 2002; 68:3076–3084. [PubMed: 12039769]

Hackstadt T, Scidmore MA, Rockey DD. Lipid metabolism in *Chlamydia trachomatis*-infected cells: directed trafficking of Golgi-derived sphingolipids to the chlamydial inclusion. Proc Natl Acad Sci USA. 1995; 92:4877–4881. [PubMed: 7761416]

Hackstadt T, Fischer ER, Scidmore MA, Rockey DD, Heinzen RA. Origins and functions of the chlamydial inclusion. Trends Microbiol. 1997; 5:288–293. [PubMed: 9234512]

Haider S, Wagner M, Schmid MC, Sixt BS, Christian JG, Häcker G, et al. Raman microspectroscopy reveals long-term extracellular activity of chlamydiae. Mol Microbiol. 2010; 77:687–700. [PubMed: 20545842]

Hatch TP, Miceli M, Silverman JA. Synthesis of protein in host-free reticulate bodies of *Chlamydia psittaci* and *Chlamydia trachomatis*. J Bacteriol. 1985; 162:938–942. [PubMed: 3997784]

Hatch TP, Miceli M, Sublett JE. Synthesis of disulfide-bonded outer membrane proteins during the developmental cycle of *Chlamydia psittaci* and *Chlamydia trachomatis*. J Bacteriol. 1986; 165:379–385. [PubMed: 3944054]

Heinz E, Tischler P, Rattei T, Myers G, Wagner M, Horn M. Comprehensive in silico prediction and analysis of chlamydial outer membrane proteins reflects evolution and life style of the *Chlamydiae*. BMC Genomics. 2009; 10:634. [PubMed: 20040079]

Heinz E, Rockey DD, Montanaro J, Aistleitner K, Wagner M, Horn M. Inclusion membrane proteins of *Protochlamydia amoebophila* UWE25 reveal a conserved mechanism for host cell interaction among the *Chlamydiae*. J Bacteriol. 2010; 192:5093–5102. [PubMed: 20675479]

Henning K, Zöller L, Hauröder B, Hotzel H, Michel R. *Hartmanella vermiformis* (*Hartmannellidae*) harboured a hidden chlamydia-like endosymbiont. Endocytobiosis Cell Res. 2007; 18:1–10.

Heuer D, Lipinski AR, Machuy N, Karlas A, Wehrens A, Siedler F, et al. *Chlamydia* causes fragmentation of the Golgi compartment to ensure reproduction. Nature. 2009; 457:731–735. [PubMed: 19060882]

Horn M. Chlamydiae as symbionts in eukaryotes. Annu Rev Microbiol. 2008; 62:113–131. [PubMed: 18473699]

Horn M, Wagner M. Bacterial endosymbionts of free-living amoebae. J Eukaryot Microbiol. 2004; 51:509–514. [PubMed: 15537084]

Horn M, Wagner M, Muller KD, Schmid EN, Fritsche TR, Schleifer KH, Michel R. *Neochlamydia hartmannellae* gen. nov., sp. nov. (Parachlamydiaceae), an endoparasite of the amoeba Hartmannella vermiformis. Microbiology. 2000; 146(Part 5):1231–1239. [PubMed: 10832651]

Horn M, Collingro A, Schmitz-Esser S, Beier CL, Purkhold U, Fartmann B, et al. Illuminating the evolutionary history of chlamydiae. Science. 2004; 304:728–730. [PubMed: 15073324]

Huang Z, Chen M, Li K, Dong X, Han J, Zhang Q. Cryo-electron tomography of *Chlamydia trachomatis* gives a clue to the mechanism of outer membrane changes. J Electron Microsc (Tokyo). 2010; 59:237–241. [PubMed: 19915209]

Hybiske K, Stephens RS. Mechanisms of host cell exit by the intracellular bacterium *Chlamydia*. Proc Natl Acad Sci USA. 2007; 104:11430–11435. [PubMed: 17592133]

Iancu CV, Tivol WF, Schooler JB, Dias DP, Henderson GP, Murphy GE, et al. Electron cryotomography sample preparation using the Vitrobot. Nat Protocols. 2006; 1:2813–2819. [PubMed: 17406539]

Kahane S, Dvoskin B, Mathias M, Friedman MG. Infection of *Acanthamoeba polyphaga* with *Simkania negevensis* and *S. negevensis* survival within amoebal cysts. Appl Environ Microbiol. 2001; 67:4789–4795. [PubMed: 11571186]

Kahane S, Fruchter D, Dvoskin B, Friedman MG. Versatility of *Simkania negevensis* infection in vitro and induction of host cell inflammatory cytokine response. J Infect. 2007; 55:e13–e21. [PubMed: 17466379]

Kahane SEM, Friedman MG. Evidence that the novel microorganism 'Z' may belong to a new genus in the family *Chlamydiaceae*. FEMS Microbiol Lett. 1995; 126:203–208. [PubMed: 7705613]

Kamneva OK, Knight SJ, Liberles DA, Ward NL. Analysis of genome content evolution in pvc bacterial super-phylum: assessment of candidate genes associated with cellular organization and lifestyle. Genome Biol Evol. 2012; 4:1375–1390. [PubMed: 23221607]

Kari L, Goheen MM, Randall LB, Taylor LD, Carlson JH, Whitmire WM, et al. Generation of targeted *Chlamydia trachomatis* null mutants. Proc Natl Acad Sci USA. 2011; 108:7189–7193. [PubMed: 21482792]

Karlsen M, Nylund A, Watanabe K, Helvik JV, Nylund S, Plarre H. Characterization of '*Candidatus Clavochlamydia salmonicola*': an intracellular bacterium infecting salmonid fish. Environ Microbiol. 2008; 10:208–218. [PubMed: 17894816]

Kostanjsek R, Strus J, Drobne D, Avgustin G. '*Candidatus Rhabdochlamydia porcellionis*', an intracellular bacterium from the hepatopancreas of the terrestrial isopod *Porcellio scaber* (Crustacea: Isopoda). Int J Syst Evol Microbiol. 2004; 54:543–549. [PubMed: 15023973]

Kremer JR, Mastronarde DN, McIntosh JR. Computer visualization of three-dimensional image data using IMOD. J Struct Biol. 1996; 116:71–76. [PubMed: 8742726]

Ladinsky, MS. Chapter eight – micromanipulator-assisted vitreous cryosectioning and sample preparation by high-pressure freezing. In: Jensen, GJ., editor. Methods in Enzymology. Amsterdam, the Netherlands: Elsevier; 2010. p. 165-194.

Ladinsky MS, Pierson JM, McIntosh JR. Vitreous cryo-sectioning of cells facilitated by a micromanipulator. J Microsc. 2006; 224:129–134. [PubMed: 17204058]

Lamoth F, Greub G. Amoebal pathogens as emerging causal agents of pneumonia. FEMS Microbiol Rev. 2010; 34:260–280. [PubMed: 20113355]

Lemcke RM. Osmolar concentration and fixation of mycoplasmas. J Bacteriol. 1972; 110:1154–1162. [PubMed: 4555408]

Lienard J, Croxatto A, Prod'hom G, Greub G. *Estrella lausannensis*, a new star in the Chlamydiales order. Microbes Infect. 2011; 13:1232–1241. [PubMed: 21816232]

Lindsay MR, Webb RI, Hosmer HM, Fuerst JA. Effects of fixative and buffer on morphology and ultrastructure of a freshwater planctomycete, *Gemmata obscuriglobus*. J Microbiol Methods. 1995; 21:45–54.

Markham AP, Jaafar ZA, Kemege KE, Middaugh CR, Hefty PS. Biophysical characterization of *Chlamydia trachomatis* CT584 supports its potential role as a type III secretion needle tip protein. Biochemistry. 2009; 48:10353–10361. [PubMed: 19769366]

Marlovits TC, Kubori T, Sukhan A, Thomas DR, Galán JE, Unger VM. Structural insights into the assembly of the type III secretion needle complex. Science. 2004; 306:1040–1042. [PubMed: 15528446]

Mastronarde DN. Automated electron microscope tomography using robust prediction of specimen movements. J Struct Biol. 2005; 152:36–51. [PubMed: 16182563]

Matsumoto A. Recent progress of electron microscopy in microbiology and its development in future: from a study of the obligate intracellular parasites, chlamydia organisms. J Electron Microsc (Tokyo). 1979; 28:57–64.

Matsumoto A. Electron microscopic observations of surface projections on *Chlamydia psittaci* reticulate bodies. J Bacteriol. 1982; 150:358–364. [PubMed: 7061397]

Matsumoto, A. Structural Characteristics of Chlamydial Bodies. Boca Raton, FL, USA: CRC Press; 1988.

Matsumoto A, Bessho H, Uehira K, Suda T. Morphological studies of the association of mitochondria with chlamydial inclusions and the fusion of chlamydial inclusions. J Electron Microsc (Tokyo). 1991; 40:356–363. [PubMed: 1666645]

Michel R, Hauröder-Philippczyk B, Müller K-D, Weishaar I. Acanthamoeba from human nasal mucosa infected with an obligate intracellular parasite. Eur J Protistol. 1994; 30:104–110.

Michel R, Müller KD, Zöller L, Walochnik J, Hartmann M, Schmid EN. Free-living amoebae serve as a host for the *Chlamydia*-like bacterium *Simkania negevensis*. Acta Protozool. 2005; 44:113–121.

Moulder JW. The relation of the psittacosis group (Chlamydiae) to bacteria and viruses. Annu Rev Microbiol. 1966; 20:107–130. [PubMed: 5330228]

Nakamura S, Matsuo J, Hayashi Y, Kawaguchi K, Yoshida M, Takahashi K, et al. Endosymbiotic bacterium *Protochlamydia* can survive in acanthamoebae following encystation. Environ Microbiol Rep. 2010; 2:611–618. [PubMed: 23766232]

Nguyen BD, Valdivia RH. Virulence determinants in the obligate intracellular pathogen *Chlamydia trachomatis* revealed by forward genetic approaches. Proc Natl Acad Sci USA. 2012; 109:1263–1268. [PubMed: 22232666]

Nichols BA, Setzer PY, Pang F, Dawson CR. New view of the surface projections of *Chlamydia trachomatis*. J Bacteriol. 1985; 164:344–349. [PubMed: 3900041]

Page, FC. An Illustrated Key to Freshwater and Soil Amoebae. Ambleside, UK: Freshwater Biological Association; 1976.

Peters J, Wilson DP, Myers G, Timms P, Bavoil PM. Type III secretion a la *Chlamydia*. Trends Microbiol. 2007; 15:241–251. [PubMed: 17482820]

Peterson EM, de la Maza LM. Chlamydia parasitism: ultrastructural characterization of the interaction between the chlamydial cell envelope and the host cell. J Bacteriol. 1988; 170:1389–1392. [PubMed: 3343223]

Pilhofer, M.; Ladinsky, MS.; McDowall, AW.; Jensen, GJ. Chapter 2 – bacterial TEM: new insights from cryo-microscopy. In: Müller-Reichert, T., editor. Methods in Cell Biology. Amsterdam, the Netherlands: Elsevier; 2010. p. 21-45.

Rockey DD, Grosenbach D, Hruby DE, Peacock MG, Heinzen RA, Hackstadt T. *Chlamydia psittaci* IncA is phosphorylated by the host cell and is exposed on the cytoplasmic face of the developing inclusion. Mol Microbiol. 1997; 24:217–228. [PubMed: 9140978]

Rourke AW, Davis RW, Bradley TM. A light and electron microscope study of epitheliocystis in juvenile steelhead trout, *Salmo gairdneri* Richardson. J Fish Dis. 1984; 7:301–309.

Roy CR. Exploitation of the endoplasmic reticulum by bacterial pathogens. Trends Microbiol. 2002; 10:418–424. [PubMed: 12217507]

Rurangirwa FR, Dilbeck PM, Crawford TB, McGuire TC, McElwain TF. Analysis of the 16S rRNA gene of microorganism WSU 86–1044 from an aborted bovine foetus reveals that it is a member of the order *Chlamydiales*: proposal of *Waddliaceae* fam. nov., *Waddlia chondrophila* gen. nov., sp. nov. Int J Syst Bacteriol. 1999; 49:577–581. [PubMed: 10319478]

Schmitz-Esser S, Toenshoff ER, Haider S, Heinz E, Hoenninger VM, Wagner M, Horn M. Diversity of bacterial endosymbionts of environmental *Acanthamoeba* isolates. Appl Environ Microbiol. 2008; 74:5822–5831. [PubMed: 18641160]

Sixt BS, Hiess B, König L, Horn M. Lack of effective anti-apoptotic activities restricts growth of *Parachlamydiaceae* in insect cells. PLoS ONE. 2012; 7:e29565. [PubMed: 22253735]

Sixt BS, Siegl A, Müller C, Watzka M, Wultsch A, Tziotis D, et al. Metabolic features of *Protochlamydia amoebophila* elementary bodies – a link between activity and infectivity in Chlamydiae. PLoS Pathog. 2013; 9:e1003553. [PubMed: 23950718]

Stone CB, Sugiman-Marangos S, Bulir DC, Clayden RC, Leighton TL, Slootstra JW, et al. Structural characterization of a novel *Chlamydia Pneumoniae*type III secretion-associated protein, Cpn0803. PLoS ONE. 2012; 7:e30220. [PubMed: 22272312]

Subtil A, Collingro A, Horn M. Tracing back to primordial chlamydiae, extinct parasites of plants? Trends Plant Sci. 2013 (in press).

Swanson MS, Isberg RR. Association of *Legionella pneumophila* with the macrophage endoplasmic reticulum. Infect Immun. 1995; 63:3609–3620. [PubMed: 7642298]

Thomas V, Casson N, Greub G. *Criblamydia sequanensis*, a new intracellular *Chlamydiales* isolated from Seine river water using amoebal co-culture. Environ Microbiol. 2006; 8:2125–2135. [PubMed: 17107554]

Tivol WF, Briegel A, Jensen GJ. An improved cryogen for plunge freezing. Microsc Microanal. 2008; 14:375–379. [PubMed: 18793481]

Wang Y, Kahane S, Cutcliffe LT, Skilton RJ, Lambden PR, Clarke IN. Development of a transformation system for *Chlamydia trachomatis*: restoration of glycogen biosynthesis by acquisition of a plasmid shuttle vector. PLoS Pathog. 2011; 7:e1002258. [PubMed: 21966270]

Wilson DP, Timms P, McElwain DL, Bavoil PM. Type III secretion, contact-dependent model for the intracellular development of chlamydia. Bull Math Biol. 2006; 68:161–178. [PubMed: 16794925]

Zheng SQ, Keszthelyi B, Branlund E, Lyle JM, Braunfeld MB, Sedat JW, Agard DA. UCSF tomography: an integrated software suite for real-time electron microscopic tomographic data collection, alignment, and reconstruction. J Struct Biol. 2007; 157:138–147. [PubMed: 16904341]

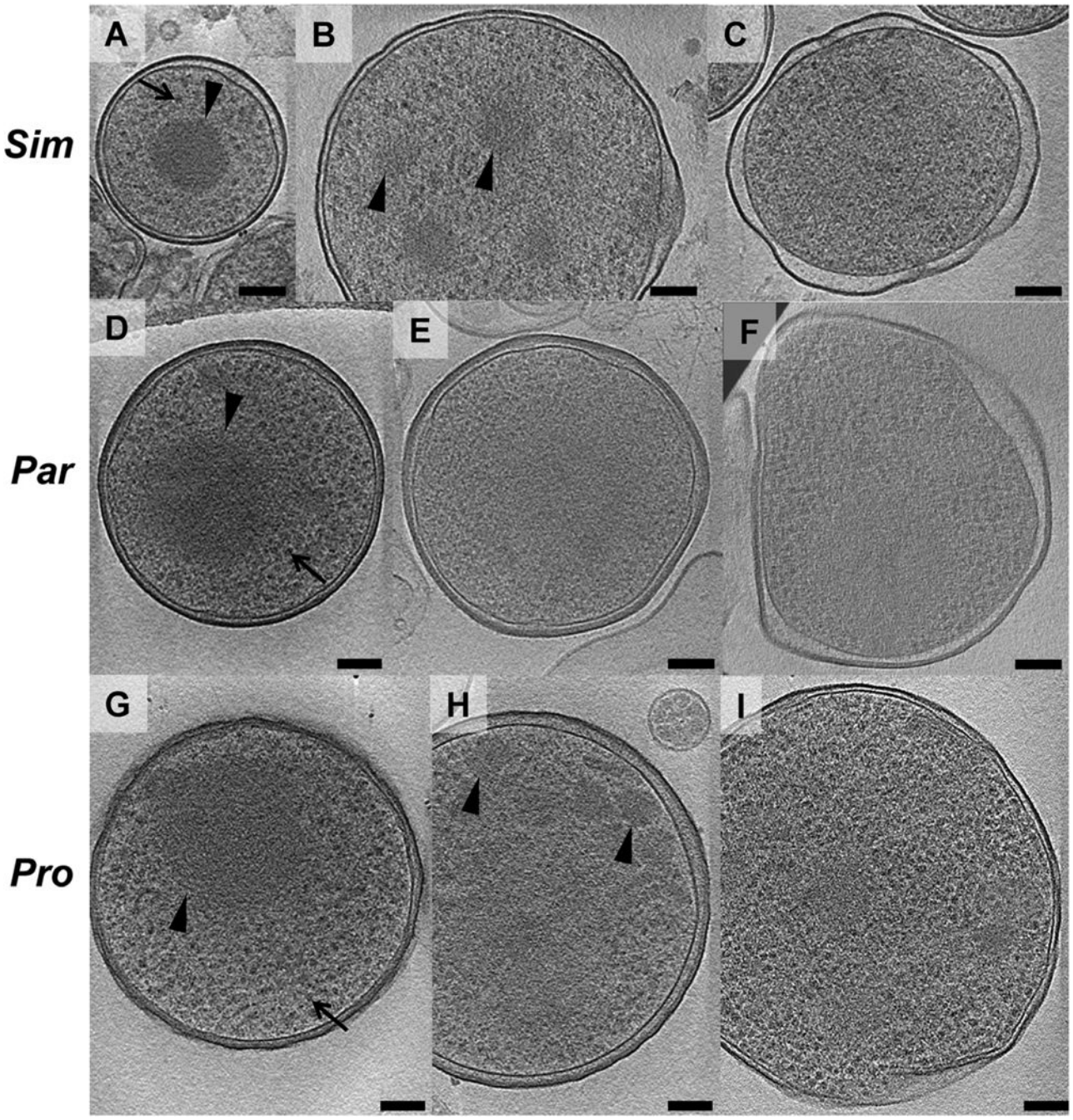

Fig. 1.

Developmental stages of environmental chlamydiae. *Simkania* (Sim, A–C), *Parachlamydia* (Par, D–F) and *Protochlamydia* (Pro, G–I) cells were purified from asynchronously infected amoeba cultures, plunge-frozen and imaged by ECT. EBs (A, D, G) and RBs (C, F, I) were identified by differences in cell size, cell shape, thickness of periplasm and cytoplasmic granularity. EBs had a smaller diameter, a spherical shape, a uniformly thin periplasm, a condensed nucleoid (arrowheads) and a large number of ribosomes (arrows). RBs had a larger cell size, a polymorphic shape, a periplasm with varying thickness, a wavier outer

membrane and a large number of ribosomes. Intermediate stages are shown in B, E, H. Shown are slices through cryotomograms. Bar, 100 nm.

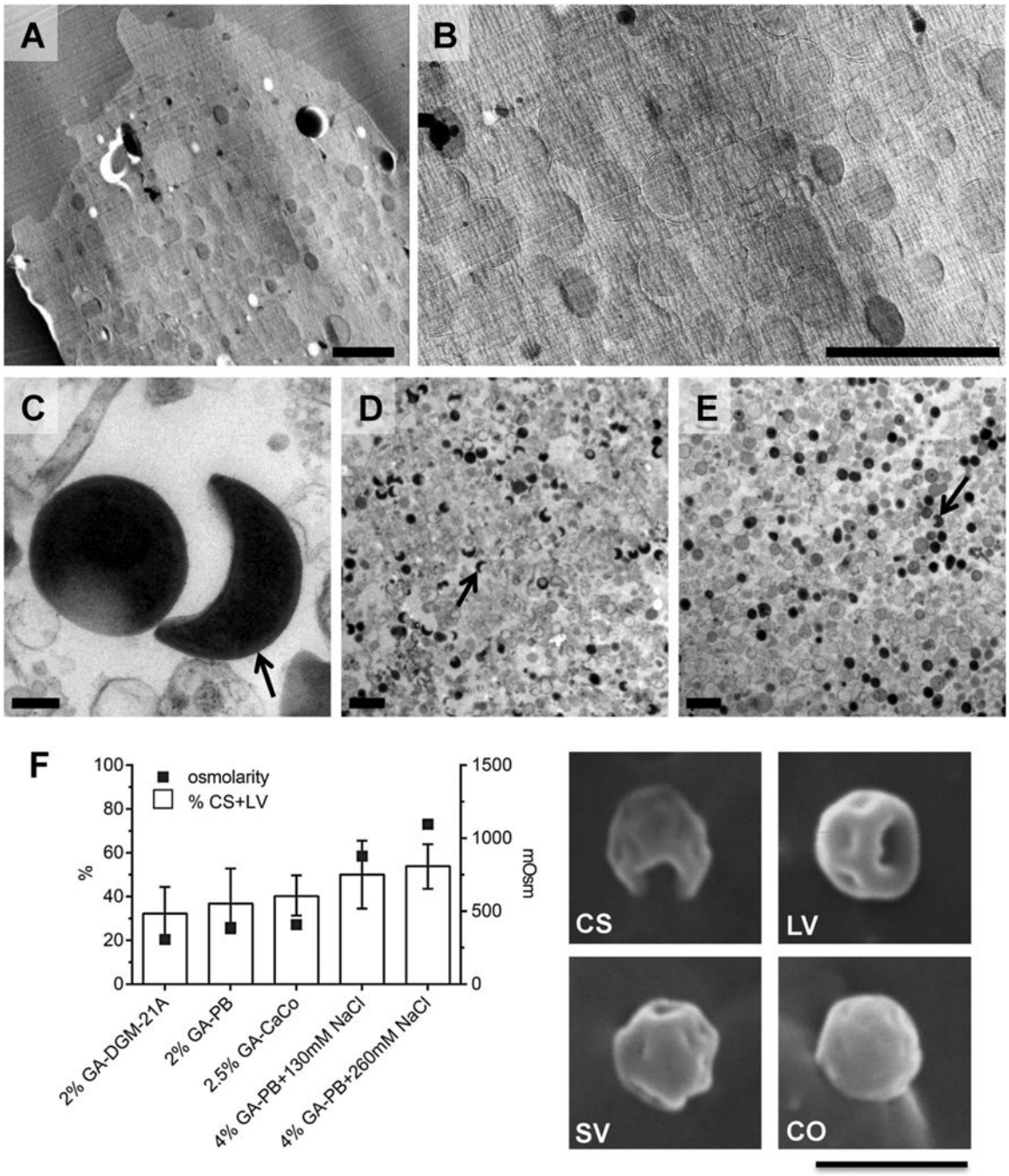

Fig. 2.

Crescent bodies are not a developmental stage but rather artefacts of conventional EM. Crescent bodies were not observed in cryotomograms of either plunge-frozen (Fig. 1, Movie S1) or cryosectioned cells (Figs 3 and 4). A two-dimensional overview image of an infected amoeba cell only showed roundish structures, representing chlamydial cells or mitochondria (A, B enlarged). In contrast, when purified *Parachlamydia* cells were fixed, dehydrated, plastic-embedded and imaged as in Greub and Raoult (2002), crescent bodies (C, D arrows) were observed frequently (47% ± 10). The use of a low-osmolarity, low-fixative

concentration buffer resulted in far fewer (2% ± 2) crescent bodies (E). Higher osmolarity and higher fixative concentration also resulted in higher percentages of crescent bodies or cells with large invaginations as observed by scanning electron microscopy (F); the graph displays the percentage of purified *Parachlamydia* cells forming crescent shapes or large invaginations after fixation with different buffers (error bars indicate the 95% confidence intervals of percentages; buffer osmolarity is indicated on the right vertical axis). Representative scanning electron microscopy images of purified *Parachlamydia* cells with different degrees of invagination are shown. CS, crescent shape; LV, large invaginations; SV, small invaginations; CO, coccoid; GA, glutaraldehyde; PB, phosphate buffer; CaCo, cacodylate buffer. Bars 2 μm (A, B, D, E, F) or 200 nm (C).

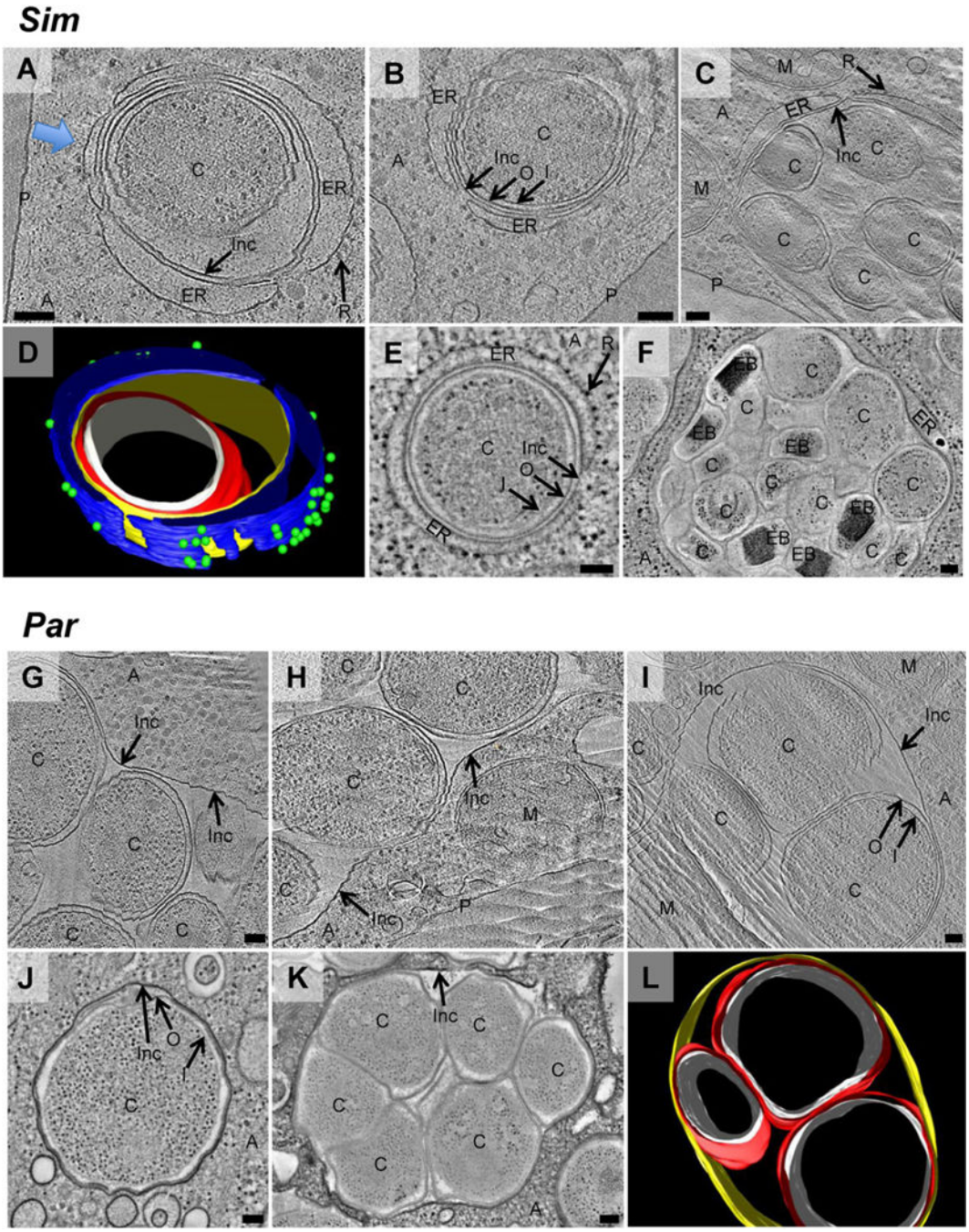

Fig. 3.

Simkania (Sim) and *Parachlamydia* (Par) form multicellular inclusions, but only *Simkania* inclusions recruit the host endoplasmic reticulum. To investigate *Simkania* (A–F) and *Parachlamydia* (G–L) inside their host, infected amoeba cultures were high-pressure-frozen, cryosectioned and imaged by ECT (cryotomographic slices are shown in A–C, G–I). For comparison, another sample was high-pressure-frozen, freeze-substituted, plastic-embedded, stained and imaged at room temperature (tomographic slices are shown in E, F, J, K). *Simkania* and *Parachlamydia* cells 'C' were found inside unicellular (A, B, E, J) and

multicellular (C, F, G, H, K, L) inclusions. Inc, inclusion membrane; I, chlamydial inner membrane; O, chlamydial outer membrane; P, amoeba plasma membrane; A, amoeba cytoplasm; M, mitochondrion. Every *Simkania* inclusion (A–F) was observed in close association with cisternae-like ribosome ('R')-studded structures, likely host rER ('ER'). The host ER almost entirely enveloped the inclusion [three-dimensional (3D) model of A in D, blue arrow indicating viewing direction; see also Movie S2]. Note that membranes in close proximity (e.g. Inc and rER membrane in E) cannot be identified as two separate membranes in conventional EM images (E, F). L is a 3D model of I (Movie S3). Colours in models: white 'I', red 'O', yellow 'Inc', blue 'ER', green 'R'. Bars, 100 nm.

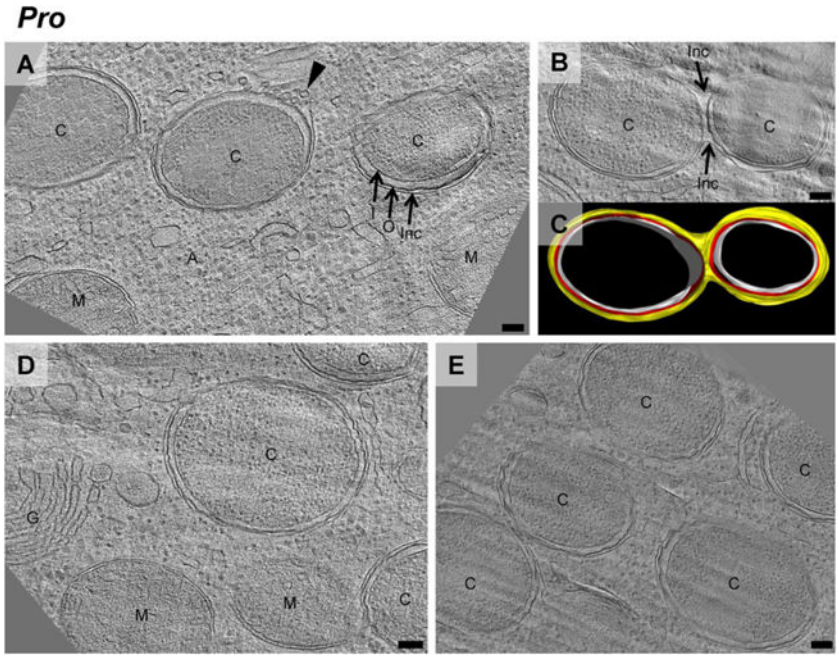

Fig. 4.

Protochlamydia (Pro) inclusions divide with chlamydial cells. (A, B, D, E) are cryotomographic slices of cryosectioned amoeba cells infected with *Protochlamydia*. In contrast with *Simkania* and *Parachlamydia*, *Protochlamydia* cells 'C' were found only inside unicellular inclusions, or in bicellular inclusions that were either in the process of division or fusion. Inc, inclusion membrane; I, chlamydial inner membrane; O, chlamydial outer membrane; P, amoeba plasma membrane; A, amoeba cytoplasm; G, golgi; M, mitochondria. In some cases, the inclusion membrane showed budding vesicles (arrowhead), suggesting more active inclusion membrane dynamics than in *Simkania* or *Parachlamydia*. C is a three-dimensional-model of B (white 'I', red 'O', yellow 'Inc'; Movie S3).

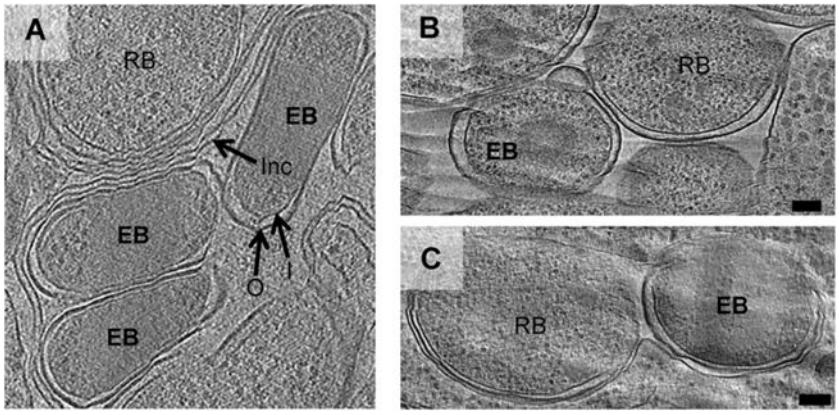

Fig. 5.

Simkania EBs show an elongated cell shape in densely packed inclusions inside the host cell. A–C show cryotomographic slices of cryosectioned amoebae infected with *Simkania*, *Parachlamydia* or *Protochlamydia* in which EBs could be identified by the granularity of the cytoplasm. In contrast with the coccoid shape of purified EBs (Fig. 1), *Simkania* EBs inside host cells (A and Fig. 3F) were sometimes elongated. *Protochlamydia* and *Parachlamydia* EBs were always coccoid, both purified (Fig. 1) and inside amoebae (B and C respectively). Bars, 100 nm.

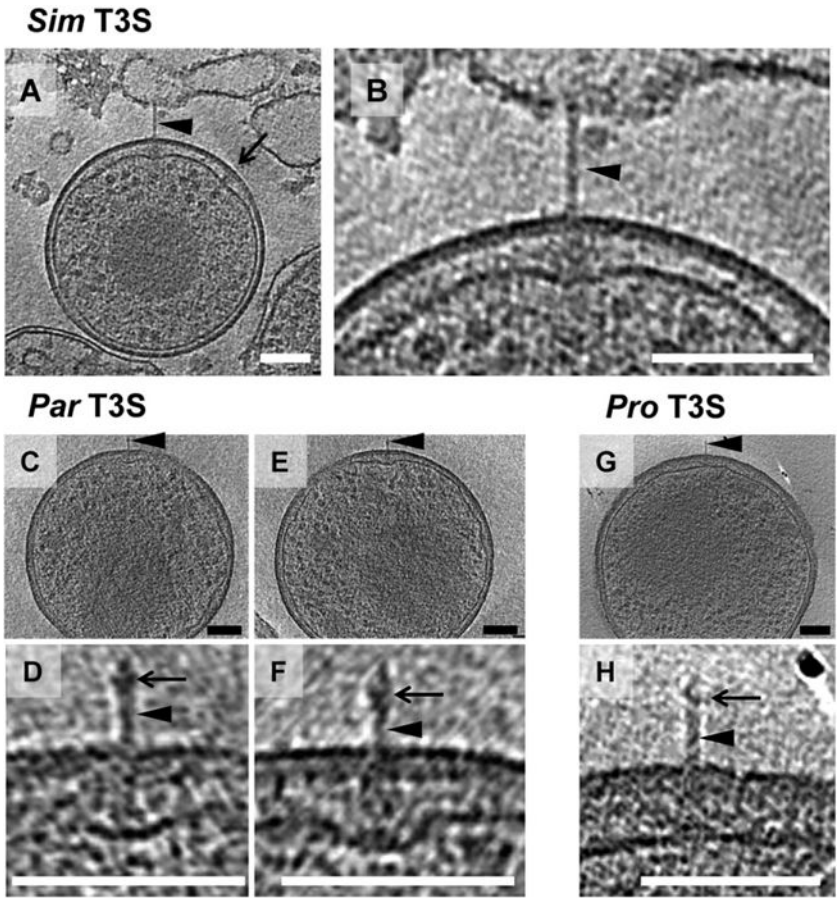

Fig. 6.

Type III secretion systems. Shown are slices through cryotomograms of purified *Simkania* (Sim) (A and B enlarged), *Parachlamydia* (Par) (C, E and D, F enlarged) and *Protochlamydia* (Pro) (G and H enlarged) EBs. All species show T3S structures (arrowheads in A–H). A pronounced widening of the periplasm was observed in *Simkania* (B) and *Parachlamydia* (D, F) to accommodate the T3S basal body. Often, such widening with periplasmic densities was observed in the absence of a needle in *Simkania* EBs (arrow in A and Fig. S2), suggesting that some needles are sheared off during purification. *Parachlamydia* and *Protochlamydia* T3S needles exhibited a bulge (arrows in D, F, H) where needle-tip proteins have been found in other bacteria.